Model Predictive Control of Bidirectional DC-DC Converters and AC/DC Interlinking Converters – A New Control Method for PV-Wind-Battery Microgrids

[1]Yinghao Shan, *Student Member, IEEE,* Jiefeng Hu, *Senior Member, IEEE,* Ka Wing Chan, *Member, IEEE,* Qing Fu, and Josep M. Guerrero, *Fellow, IEEE*

***Abstract*—In renewable energy systems, fluctuating outputs from energy sources and variable power demand may deteriorate the voltage quality. In this paper, a model predictive control strategy without using any proportional-integral-derivative (PID) regulators is proposed. The proposed strategy consists of a model predictive current and power (MPCP) control scheme and a model predictive voltage and power (MPVP) control method. By controlling the bidirectional dc-dc converter of the battery energy storage system based on the MPCP algorithm, the fluctuating output from the renewable energy sources can be smoothed, while stable dc-bus voltage can be maintained. Meanwhile, the ac/dc interlinking converter is controlled by using the MPVP scheme to ensure stable ac voltage supply and proper power flow between the microgrid and the utility grid. Then, a system-level energy management scheme (EMS) is developed to ensure stable operation under different operation modes by considering fluctuating power generation, variable power demand, battery state of charge (SOC), and electricity price. Compared with the traditional cascade control, the proposed method is simpler and shows better performance, which is validated in simulation based on a 3.5 MW pv-wind-battery system with real-world solar and wind profiles.**

***Index Terms*—Hybrid ac/dc microgrids, energy storage, coordinated control**

I. Introduction

For decades, cascade linear control has dominated the power electronic control techniques. However, this approach has major drawbacks [1]. First, the control structure is complicated with multiple feedback loops and PWM modulation, which leads to slow dynamic response. Second, the tuning of the proportional-integral-differential (PID) parameters is time-consuming, which makes the controller not easy to implement. In a practical microgrid, fluctuating output from renewable energy sources can cause oscillations in dc-bus voltage, which in turn, may further deteriorate the power quality on the ac side. As a result, traditional cascade control may no longer be effective to deal with this fluctuation.

In microgrids with multiple energy sources and converters, to achieve load sharing between distributed generation units (DGs), inner current and outer voltage feedback loop control is commonly incorporated with droop method [2], [3]. In the last few years, much research efforts have been paid to obtain satisfactory and good performance by using traditional PID methods for ac microgrids. For example, by introducing power derivative-integral terms into a conventional droop together with inner voltage/current feedback loops, fast transient response in power sharing between inverters can be achieved [4]. Adaptive virtual impedance is proposed to achieve good performance for the reactive power sharing nonlinear loads [5]. By combing the virtual impedance and secondary control, the active and reactive powers can be shared with mismatched feeder impedance [6]. The effectiveness of droop function may however be deteriorated by incorporating such cascade linear control.

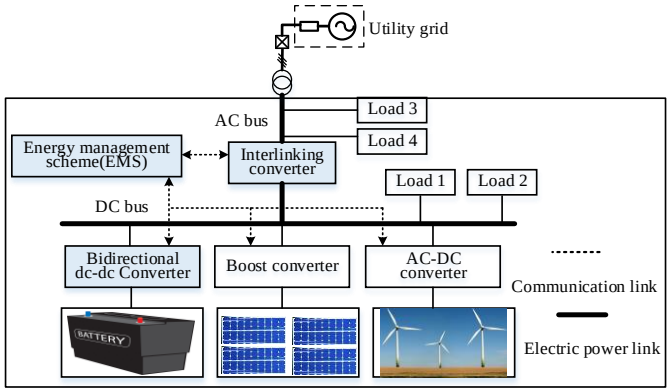

Fig. 1 A microgrid with multiples energy sources and converters.

Recently, due to the increasing presence of dc power sources in microgrids such as PV, fuel-cell, energy storages, modern dc loads, and considering the existing century-long ac power systems, interests on hybrid ac/dc microgrids are growing rapidly [7]-[12]. Traditionally, cascade inner current and outer voltage feedback loop with PID regulators are commonly used to control dc-dc converters and ac/dc interlinking converters in such microgrids. Typically, in islanded mode, the main ac/dc interlinking converter is controlled to provide a stable voltage and frequency for the ac subgrid while the dc-link voltage is maintained by the bidirectional dc-dc converter [7]-[9]. In grid-connected mode, the ac/dc interlinking converter is used to maintain a stable dc-link voltage and to exchange power between the microgrid and the utility system [10]-[12]. As the dc-dc converters and the ac/dc interlinking converters are vital to ensure stable dc and ac supply, the drawbacks of the conventional cascade control with PID regulators may affect the voltage quality.

[1] This work was supported in part by The Hong Kong Polytechnic University under Grant (1-ZE7J), Hong Kong Research Grants Council under Grant (PolyU252040/17E) and Science and Technology Development Foundation of Guangdong Province under Grants (2017A050506023, 2016B090918107) (*Corresponding author: J Hu*)

Y. Shan, J. Hu, and K.W. Chan are with the Department of Electrical Engineering, The Hong Kong Polytechnic University, Hung Hom, Hong Kong (e-mail: yh.shan@connect.polyu.hk; jerry.hu@polyu.edu.hk; kevin.kw.chan@polyu.edu.hk).

Q. Fu is with the School of Physics, Sun Yat-sen University, Guangzhou 510006, China (e-mail: fuqing@mail.sysu.edu.cn)

J. M. Guerrero is with the Department of Energy Technology, Aalborg University, Aalborg DK-9220, Denmark (e-mail: joz@et.aau.dk)

Another concern is that, in existing microgrid research, the inputs of the distributed inverters are usually connected to ideal dc power sources to simulate a variety of renewable energy resources. For control techniques development of inverters, it is reasonable and sufficient because this assumption can facilitate the design process. From the viewpoint of practical applications, however, the intermittent nature of such energy resources must be considered. Under variable power generation and power demand conditions, the traditional cascade control methods may no longer be effective to deal with this fluctuation. More advanced control methods may be therefore required to ensure stable operation and high power quality.

In the last few years, the model predictive control (MPC) scheme, in which the optimal switching state of the power converter is determined according to a specified cost function, has been adopted to obtain better performance [13]-[16]. Still, MPC is seldom reported in the coordinated control of multiple converters in microgrids, although some system-level algorithms have been proposed to achieve a variety of goals such as minimizing system operating costs [17], optimized power flow management [18] and economic load dispatch [19]. These algorithms are designed and implemented at the system level. Nevertheless, the structures of the microgrids and the control of power converters have not been considered. Meanwhile, device-level MPC has also been investigated in microgrids. For example, a MPC strategy is proposed to control the converter of the energy storage system (ESS) to smooth the PV output and stabilize the dc-bus voltage [20]. This PV-ESS configuration is very simple. Comprehensive operation of the microgrid and the power management system are not considered. In [21], a MPC approach is combined with droop method to control parallel-inverter ac microgrid. However, intermittent nature of the renewable energy resources is not considered. In this sense, the question now becomes: In renewable energy based microgrids with multiple power converters as interfaces, is it possible to replace all the traditional cascade voltage or current feedback loops by using MPC approaches; And, to what extent, the overall system performance can be improved.

In this paper, a new control strategy based on MPC is developed for renewable energy based microgrids. The topology of the microgrid is shown in Fig. 1. The renewable energy resources could be the wind, solar, wave, etc [22], [23], [24]. Here, solar PV system and wind generator are adopted as an example, which is not the main focus in this research. There are two parts in the whole system: DC subgrid with dc loads and ac subgrid with ac loads. The battery energy storage system (BESS) is connected to the dc bus via a dc/dc converter. The ac and dc buses are interconnected through a bidirectional ac/dc interlinking converter which is a three-phase two-level voltage source inverter (VSI). A model predictive current and power (MPCP) scheme is developed to control the bidirectional dc-dc converter in the BESS, while a model predictive voltage and power (MPVP) method is proposed to control the ac/dc interlinking converter. They are used to coordinately control the dc/dc converter and ac/dc converter to smooth the renewable energy outputs and maintain dc- and ac-buses voltages. Finally, by considering practical aspects such as fluctuating power generation, variable power demand, battery state of charge (SOC), electricity price, etc., an energy management scheme (EMS) is developed to ensure stable operation under different operation modes. Our contributions in this work are highlighted as follows.

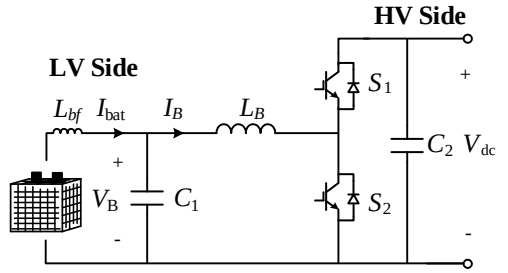

Fig. 2. Schematic diagram of the battery energy storage system (BESS).

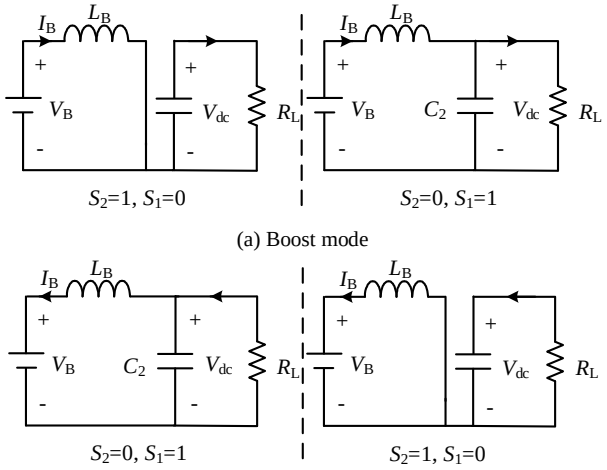

Fig. 3. Topologies of boost mode and buck mode.

1) Compared with traditional cascade linear control, the proposed scheme avoids PID parameters tuning, PWM modulation and complex coordinate transformation.

2) By using proposed MPC scheme, the dc-bus voltage can be better maintained with less oscillations and overshoots under fluctuating power generation and consumption profiles. Meanwhile, the ac-bus voltage has a better quality with less harmonic interferences.

3) A comprehensive system-level power management scheme in consideration of fluctuating power generation, variable power demand, battery state of charge (SOC), and electricity price is developed to ensure stable operation and steady transition under different operation modes.

II. MPCP of Bidirectional Buck-boost Converter

The aim of the BESS is to compensate the power gap caused by the renewable energy sources and the load demand. Since the power supplied or absorbed by BESS is actually controlled by switching the buck-boost converter, it is necessary to obtain the effect of its switching states on the power supplied/absorbed. Fig. 2 shows the circuit of the BESS. L_{bf} is the battery filter to reduce the current ripple [25], V_B means the battery voltage, V_{dc} the dc bus voltage, I_{bat} battery output current and I_B inductor current. The converter has two sides, low voltage (LV) bus and high voltage (HV) bus. They are connected to the battery and the common dc bus, respectively. Switches S_1 and S_2 are driven by a set of complementary signals. When battery discharges to supply power, the BESS operates in boost mode (Fig.3 (a)). On the contrary, when battery is charged to absorb power, the BESS operates in buck mode (Fig.3 (b)).

Combining (a) and (b) of Fig.3 and defining I_B in boost mode as a positive current, ultimately we have only two states:

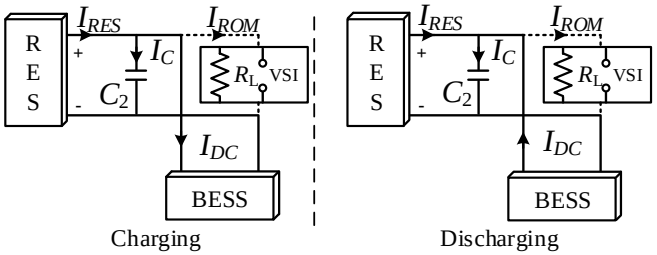

Fig. 4. Illustration of the currents flow within the system.

$$\begin{cases} S_2=1, S_1=0: \ L_B\dfrac{dI_B}{dt}=V_B \\ S_2=0, S_1=1: \ L_B\dfrac{dI_B}{dt}=V_B-V_{dc} \end{cases} \tag{1}$$

The discrete-time model for a sampling time T_s can be expressed as:

$$\begin{cases} S_2=1, S_1=0: \ I_B(k+1)=\dfrac{T_s}{L_B}V_B(k)+I_B(k) \\ S_2=0, S_1=1: \ I_B(k+1)=\dfrac{T_s}{L_B}(-V_{dc}(k)+V_B(k))+I_B(k) \end{cases} \tag{2}$$

To charge or discharge the battery, the following cost function can be formulated to regulate the battery current.

$$\begin{aligned} &J_c=\left|I_B^*-I_B(k+1)\right| \\ &s.t.\ SOC_{\min}\le SOC\le SOC_{\max},\ I_B\le\left|I_{bat\_rated}\right| \end{aligned} \tag{3}$$

where I_B^* is the battery current reference which is set according to the electricity price in grid-connected operation, which will be explained further in Section IV.

Fig. 4 illustrates the currents flow between the renewable energy sources (RES), BESS and the rest of the microgrid (ROM). To keep the power balance within the microgrid, the BESS should discharge and be charged properly. By applying Kirchoff's current law (KCL), the relationship of the currents can be expressed as:

$$I_{DC}=I_{RES}-I_C-I_{ROM} \tag{4}$$

where I_{DC} denotes the current supplied or absorbed by BESS, I_{RES} the current from the renewable energy sources, I_C the current flowing through the dc-side capacitor, I_{ROM} the current following into dc loads and the inverter. Consequently, the (k+1)th required power by BESS to keep the power balance within the microgrid can be calculated as

$$P_{BESS}^*(k+1)=\left|I_{DC}(k+1)\cdot V_{dc}^*\right| \tag{5}$$

where V_{dc}^* is the voltage reference for dc bus.

As can be seen in Fig. 2, the dc side voltage V_{dc} relates directly

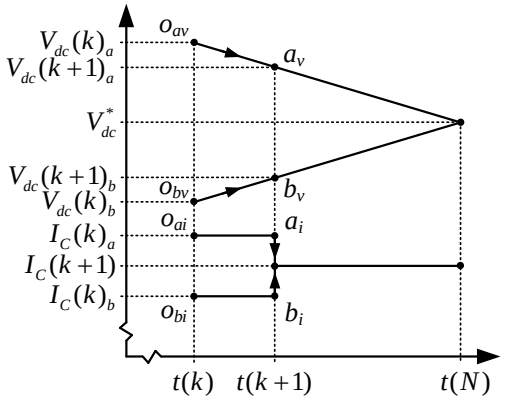

Fig. 5. Next instant reference design.

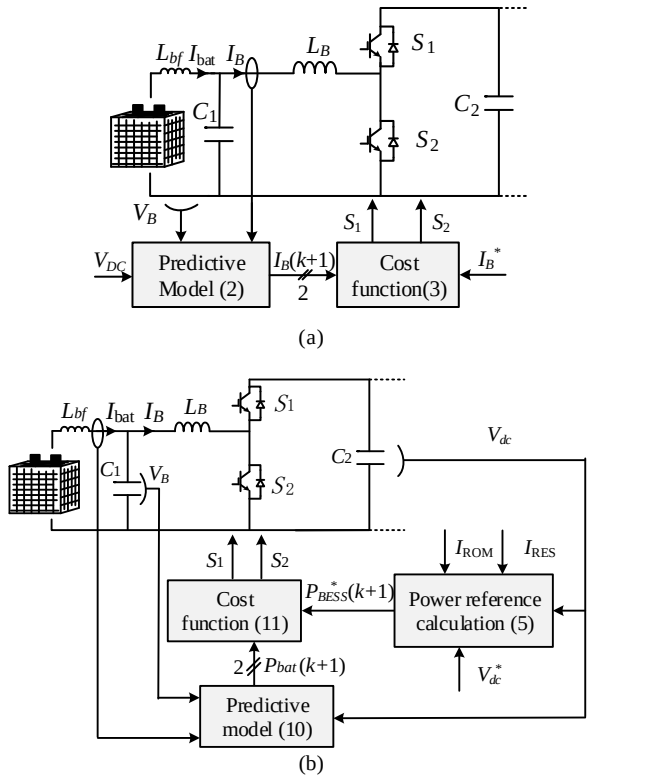

Fig. 6. Block diagram of MPCP to control buck-boost converters. (a) operation in grid-connected mode, (b) operation in islanded mode.

to the effect of capacitor C_2. For a certain capacitor, it's known that the capacitor voltage can be determined by the current flowing through it (I_C), that is $I_C = C_2 dV_{dc}/dt$. From this equation, one can obtain that the change of dc side voltage V_{dc} can result in corresponding change of the current I_C. Whilst V_{dc} is desired to be controlled around its rated value V_{dc}^*, this means there is always a deviation between V_{dc} and V_{dc}^*. Here, we assume the deviation obeys a linear change within a short period, as illustrated in Fig. 5. Considering I_C value decided by the V_{dc} gap cannot be randomly large, a reference prediction horizon N is introduced [14].

In Fig. 5, at present moment, $V_{dc}(k)$ may be higher ($V_{dc}(k)_a$) or lower ($V_{dc}(k)_b$) than the rated dc voltage V_{dc}^*, so it needs to decrease (from o_{av} to a_v) or increase (from o_{bv} to b_v) respectively to approximate its desired final value V_{dc}^*. Accordingly, this process results in $I_C(k)_a$ steps down or $I_C(k)_b$ steps up. N means $V_{dc}(k)$ will achieve V_{dc}^* in N steps. Just taking next instant k+1 into account, it can be obtained that [14]

$$\frac{V_{dc}(k)-V_{dc}(k+1)}{1}=\frac{V_{dc}(k)-V_{dc}^*}{N} \tag{6}$$

Put it further

$$V_{dc}(k+1)=V_{dc}(k)+\frac{1}{N}(V_{dc}^*-V_{dc}(k)) \tag{7}$$

Similarly, when Euler's forward-difference law works

$$I_C(k+1)=\frac{C_2}{T_s}(V_{dc}(k+1)-V_{dc}(k))=\frac{C_2}{NT_s}(V_{dc}^*-V_{dc}(k)) \tag{8}$$

where N also works as an integer coefficient used to limit the capacitor's current. According to (4) and (8), BESS current can be predicted as

$$I_{DC}(k+1)=I_{RES}(k)-I_C(k+1)-I_{ROM}(k) \tag{9}$$

Considering the relatively slow change of the battery voltage V_B (i.e. $V_B(k)=V_B(k+1)$) and the equality of battery output current I_{bat} and inductor current I_B in steady state, the battery output power can be predicted as

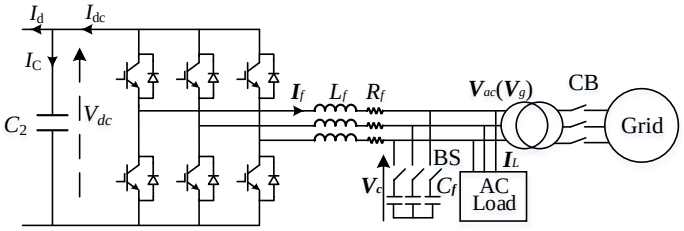

Fig. 7 AC side of the microgrid

$$P_{bat}(k+1) = \left| I_B(k+1) \cdot V_B(k) \right| \tag{10}$$

The required power of the BESS to keep the power balance with the microgrid should be provided by the battery through the buck-boost converter. Therefore, the following cost function should be minimized

$$\begin{aligned} J_P &= \left| P^*_{BESS}(k+1) - P_{bat}(k+1) \right| \\ s.t.\ SOC_{\min} &\le SOC \le SOC_{\max},\ I_B \le \left| I_{bat\_rated} \right| \end{aligned} \tag{11}$$

Fig. 6 illustrates the proposed MPCP strategy. In grid-connected mode, to directly control the charging or discharging current of the battery, the battery voltage and current, together with the actual dc-bus voltage, will be used to predict the battery current $I_B(k+1)$ according to (2). Then, the switching behavior that minimizes (3) will be selected to control the buck-boost converter. In islanded mode, the BESS is used to maintain a constant dc-bus voltage. The renewable energy sources output current, I_{RES}, the current following into dc loads and the inverter for ac loads, I_{ROM}, actual dc-bus vo ltage V_{dc} and reference voltage V_{dc}^*, are first used to calculate the required BESS power according to (5), (8) and (9). Meanwhile, the battery voltage and current, together with the actual dc-bus voltage, will be used to predict the battery current $I_B(k+1)$, leading to two possible values of $P_{bat}(k+1)$ according to (2) and (10). Then, the switching behavior that minimizes (11) will be selected to control the buck-boost converter. In this way, the dc-bus voltages can be maintained stable as common dc link for distributed generations and as dc input for the dc/ac interlinking inverter.

III. MPVP OF AC/DC INTERLINKING CONVERTER

Every leg of the VSI contains two switches which can employ number 1/0 to symbolize their ON/OFF respectively. Switching actions (i.e. decision variables) affect the output voltage of inverters (V_0, V_1, …, V_7), and there are corresponding eight possible switching states (000, 100, 110, 010, 011, 001, 101, and 111). Possible converter voltage vectors $\boldsymbol{V}_i$ can be expressed as

$$\boldsymbol{V}_i = \begin{cases} \dfrac{2}{3} V_{dc} e^{j(i-1)\frac{\pi}{3}} & (i = 1, 2, \cdots, 6) \\ 0 & (i = 0, 7) \end{cases} \tag{12}$$

Fig. 7 describes the ac subgrid. In grid-connected mode, the circuit breaker (CB) is turned ON and the bypass switch (BS) is switched OFF. The mathematical model can be expressed as

$$\boldsymbol{V}_i = \boldsymbol{V}_g + \boldsymbol{I}_f R_f + L_f \frac{d\boldsymbol{I}_f}{dt} \tag{13}$$

where $\boldsymbol{V}_g$ is the grid voltage vector, $\boldsymbol{I}_f$ the inductor current vector, L_f the filter inductance; R_f the equivalent resistance. The output active and reactive powers of the ac/dc interlinking converter are

$$P = \frac{3}{2} \mathrm{Re}\left\{ \boldsymbol{V}_g \bar{\boldsymbol{I}}_f \right\} = \frac{3}{2} \left(V_{g\alpha} I_{f\alpha} + V_{g\beta} I_{f\beta} \right) \tag{14}$$

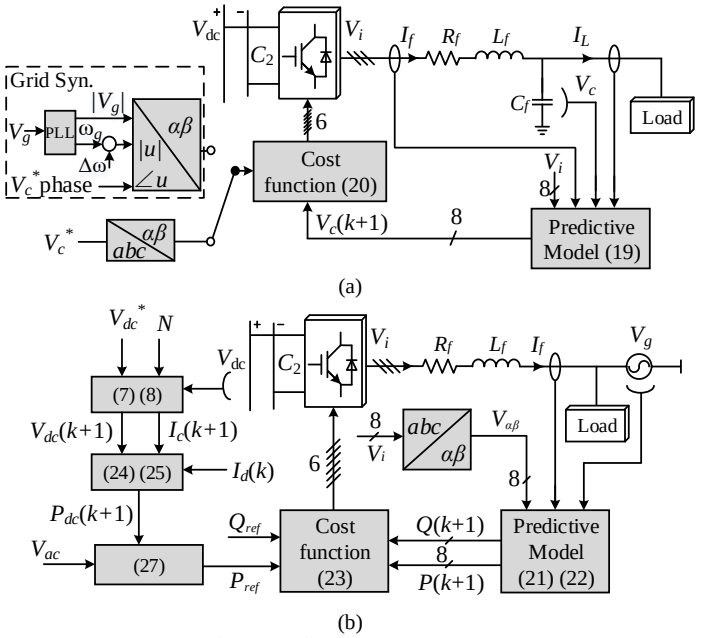

Fig. 8 Block diagram of MPVP of AC/DC interlinking converters. (a) islanded operation, (b) grid-connected operation.

$$Q = \frac{3}{2} \mathrm{Im}\left\{ \boldsymbol{V}_g \bar{\boldsymbol{I}}_f \right\} = \frac{3}{2} \left(V_{g\beta} I_{f\alpha} - V_{g\alpha} I_{f\beta} \right) \tag{15}$$

where '$^-$' is the complex conjugate operation. In islanded operation, the CB is turned OFF and the BS is switched ON. In this case, the dynamic behavior of the capacitor of the *LC* filer can be expressed as

$$C \frac{d\boldsymbol{V}_c}{dt} = \boldsymbol{I}_f - \boldsymbol{I}_L \tag{16}$$

where $\boldsymbol{V}_c$ is the capacitor voltage vector (i.e. the load voltage vector), C_f the filter capacitance, $\boldsymbol{I}_L$ the load current vector. The mathematical model of the ac/dc interlinking converter can be described as

$$\boldsymbol{V}_i = \boldsymbol{I}_f R_f + L_f \frac{d\boldsymbol{I}_f}{dt} + \boldsymbol{V}_c \tag{17}$$

A. Islanded Operation

Fig. 8(a) depicts the block diagram of the proposed MPVP strategy of AC/DC converters. In islanded operation, the dc-bus voltage can be maintained by the BESS. The ac/dc interlinking converter, like the uninterruptible power supply (UPS), is used to provide a stable ac voltage for the ac load. With this goal, the capacitor voltage should be the control objective of the MPVP controller. Combining (16) and (17), the system model can be rewritten as a state-space system [26], [27]

$$\frac{d\boldsymbol{x}}{dt} = A\boldsymbol{x} + B\boldsymbol{y} \tag{18}$$

where

$$\boldsymbol{x} = \begin{bmatrix} \boldsymbol{V}_c \\ \boldsymbol{I}_f \end{bmatrix}, \quad \boldsymbol{y} = \begin{bmatrix} \boldsymbol{V}_i \\ \boldsymbol{I}_L \end{bmatrix}, \ A = \begin{bmatrix} 0 & 1/C_f \\ -1/L_f & -R_f/L_f \end{bmatrix},$$

$$B = \begin{bmatrix} 0 & -1/C_f \\ 1/L_f & 0 \end{bmatrix},$$

By solving the linear differential equation of (18), it can be expressed in discrete-time form as [28]

$$\boldsymbol{x}(k+1) = e^{T_s A} \boldsymbol{x}(k) + A^{-1}(e^{T_s A} - \boldsymbol{I}_{2\times 2}) B \boldsymbol{y}(k) \tag{19}$$

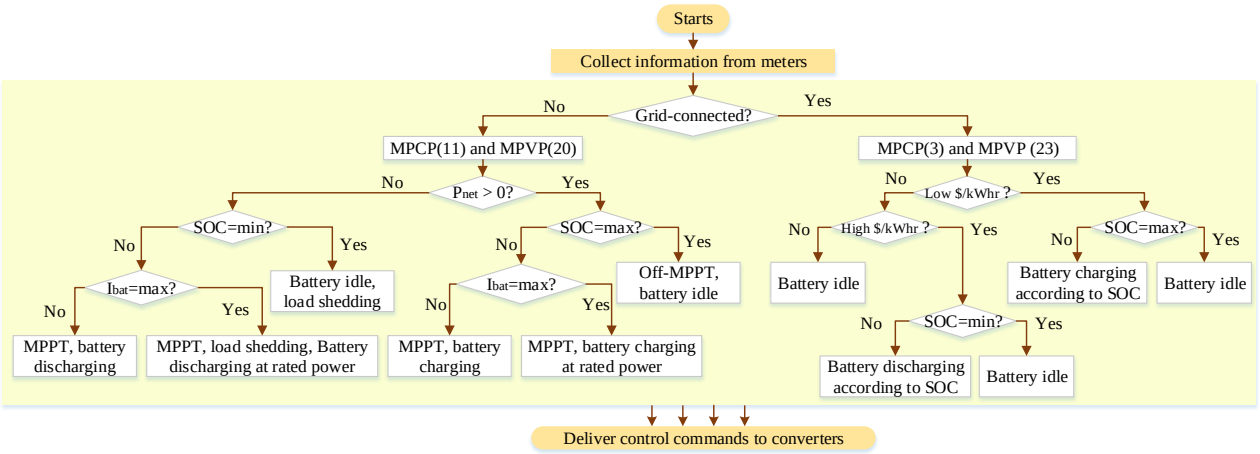

Fig. 9 System-level control for energy management.

Therefore, the capacitor voltage at (k+1)th instant can be predicted according to (19). To control the capacitor voltage tightly, the cost function is formulated to

$$J_V = \left(V_{c\alpha}^{ref} - V_{c\alpha}^{k+1}\right)^2 + \left(V_{c\beta}^{ref} - V_{c\beta}^{k+1}\right)^2 \tag{20}$$

Based on this cost function, the voltage vector that generates the least value of J_V will be applied during the next sampling period. Because the α and β components are tightly controlled, the $\boldsymbol{V}_c$ can track its reference. Thus stable and sinusoidal voltage can be established.

In Grid synchronization, phase-locked loop (PLL) is used to obtain the grid voltage amplitude and frequency. Then, a voltage with the same amplitude and a slightly higher frequency is set as the voltage reference for the cost function (20). Aslo, the phase of this voltage reference is set as the same as that of V_c^* in previous islanded operation. In this way, the microgrid ac voltage phasor and grid voltage phasor will rotate in different angular speeds but with same amplitudes. Once the phase angle of the microgrid ac voltage is aligned with that of the grid voltage, grid connection can be conducted.

B. Grid-connected operation

In grid-connected mode, the ac/dc interlinking converter is used to maintain a stable dc-bus voltage for dc loads and to exchange power between the microgrid and the utility grid. When resource conditions or load capacities change, the dc bus voltage is adjusted to constant so as to keep the power balance within the system. The active and reactive powers at the end of a sampling period can be predicted from (13), (14) and (15) as

$$P(k+1) = T_s\left[-\frac{R_f}{L_f}P(k) - \omega Q(k) + \frac{3}{2L_f}\left(\left|\boldsymbol{V}_g\right|^2 - \mathrm{Re}\left(\boldsymbol{V}_g\bar{\boldsymbol{V}}_i\right)\right)\right] + P(k) \tag{21}$$

$$Q(k+1) = T_s\left[\omega P(k) - \frac{R_f}{L_f}Q(k) - \frac{3}{2L_f}\mathrm{Im}\left(\boldsymbol{V}_g\bar{\boldsymbol{V}}_i\right)\right] + Q(k) \tag{22}$$

where ω is the grid frequency in radians. Since the control objectives in grid-tied mode are the active and reactive powers. Therefore, we can evaluate the effects of each voltage vector on P and Q and select the one minimizing the following cost function

$$J_P = \left(P_{ref} - P(k+1)\right)^2 + \left(Q_{ref} - Q(k+1)\right)^2 \tag{23}$$

Usually, in order to maintain a unity power factor, the reactive power setting is expected to be set to null, i.e. Q_{ref} = 0Var. From this point, the remaining variable in cost function that needs to be determined is the active power reference P_{ref}.

Then, applying KCL at the circuit shown in Fig. 7, and similar to (9), one can obtain

$$I_{dc}(k+1) = I_C(k+1) + I_d(k) \tag{24}$$

Thus, the power on dc side can be calculated by

$$P_{dc}(k+1) = V_{dc}(k+1)I_{dc}(k+1) \tag{25}$$

It is noted that the dc side power is linked to the ac side power, defining it as $P_{ac}(k+1)$. Considering the power loss of the power lines between the converter and the utility grid, the following relationship can be derived

$$P_{ac}(k+1) - \frac{2}{3}\left(\frac{P_{ac}(k+1)}{V_{ac}}\right)^2 R_f = P_{dc}(k+1) \tag{26}$$

where V_{ac} is the ac source voltage amplitude. Solve this equation, we get the following equation which is also the reference active power P_{ref} in the cost function.

$$P_{ac}(k+1) = \frac{3V_{ac}^2}{4R}\left(1 - \sqrt{1 - \frac{8R}{3V_{ac}^2}P_{dc}(k+1)}\right) = P_{ref} \tag{27}$$

After the power references are obtained, the system model is used to predict the powers at next sampling instant. A cost function is then employed as the criterion to select the optimum voltage vector of the converter. Finally, the voltage vector that can minimize the cost function is applied, as depicted in Fig. 8(b).

IV. System Level Control

In this section, the system-level control is developed. The overall control for energy management is illustrated in Fig. 9. The power within the microgrid should be balanced as follows [8]

$$P_{pv} + P_w + P_{bat} + P_g - P_{loss} = P_{acL} + P_{dcL} \tag{28}$$

where P_{pv} is the output power of the PV system, P_w the output power of the wind generation system, P_{bat} the battery power, P_g the power exchanging with utility grid, P_{loss} the total power loss, P_{acL} implies the power of ac loads, P_{dcL} the power of dc loads. P_{net} is defined as P_{pv} and P_w subtracted by P_{acL}, P_{dcL} and P_{loss}. Positive P_{bat} indicates discharging while negative represents charging. Positive P_g means drawing power from utility and negative indicates injecting power to utility.

A. Mode 1 operation

This mode refers to grid-connected operation. Any power surplus or deficit within the microgrid is automatically balanced by the ac distribution network. The ac/dc interlinking converter operates in MPVP scheme to maintain the dc-bus voltage to

TABLE I System Parameters

Description	Value
Solar PV	SunPower Spr-305E-WHT-D, 2.8 MW
Wind turbine	Base wind speed 12m/s, R=31m, C_p=0.47
PMSG	1.5 MW, L_d=L_q=0.3mH, Φ_V=1.48Wb, p = 48
ESS	Lithium-Ion battery, 1 MW, 300V, 1.3 kA·h, L_{bf}=50μH
DC-bus voltage	1.2 kV
DC-bus capacitor	20 mF
AC-bus voltage	25 kV / 0.69 kV 60Hz
AC-bus LC filter	L = 0.6mH, C=1338μF, R=1.9mΩ
Linear loads	Critical load 1 – 1MW, non-critical load 2 – 0.5MW
Non-linear loads	Critical load 3 – 1MW, non-critical load 4 – 0.5MW
PI gains of traditional method	
BESS grid-tied	Current loop: k_p=1.5, k_i=1 (f_{sw} = 2kHz)
BESS islanded	Outer voltage loop: k_p=10, k_i=50 Inner current loop: k_p=5, k_i=2 (f_{sw} = 2kHz)
Interlinking converter grid-tied	Outer voltage loop: k_p=5, k_i=600 Inner current loop: k_p=4, k_i=20 (f_{sw} = 10kHz)
Interlinking converter islanded	Outer voltage loop: k_p=46, k_i=0 Inner current loop: k_p=7, k_i=0 (f_{sw} = 3kHz)

TABLE II Events during grid-connected operation.

Events	Operations	Time (s)
1	Wind speed step down	5
2	Load 3 switched in	8
3	Load 2 switched in	11
4	Load 4 switched in	13
5	Wind speed step up	15
6	Load 1 switched off	17

transfer the power between the dc subgrid and ac subgrid. In this case, the PV and wind generator should produce as much power as possible for the microgrid and the utility. Also, no load shedding is required and the ESS can be charged or discharged depending on the actual electricity price. Here, a hysteresis-like control with a "deadband" in the middle is adopted. If the electricity price \$/kWhr is lower than a specified level (lower limit), the ESS is charged to store energy. Inversely, if the electricity price is higher than another specified level (upper limit), the ESS discharges to supply energy to avoid expensive electricity bill. Otherwise, the ESS will be in idle mode without any action. Furthermore, to avoid overcharge or overdischarge, the charging/discharging rate (i.e., the battery current reference) varies with the SOC linearly [29]. Take the charging mode for example, the higher the SOC is, the slower the charging rate becomes. When the SOC reaches the maximum value, I_{bat} becomes zero to avoid overcharge.

B. Mode 2 operation

This mode refers to islanded operation. Since the hybrid microgrid becomes an isolated system, the power needs to be balanced within the microgrid. In this case, the dc-bus voltage is maintained by the ESS. The ac-bus voltage is established by the ac/dc interlinking converter using MPVP scheme. Specifically, there are two conditions that need to be considered.

1) Low wind and irradiation and heavy load

Under this scenario, the generation from PV and wind cannot meet the load demand. As a result, both the PV and wind generator should operate in MPPT while the ESS provides additional power by battery discharging. If the required power by the ESS exceeds the power rating of the battery or the SOC drops down to the minimum value, load shedding becomes necessary to guarantee power supply to the most critical loads. For example, in a residential microgrid network, critical loads include equipment in hospitals and data centers. Non-critical loads could be the electric

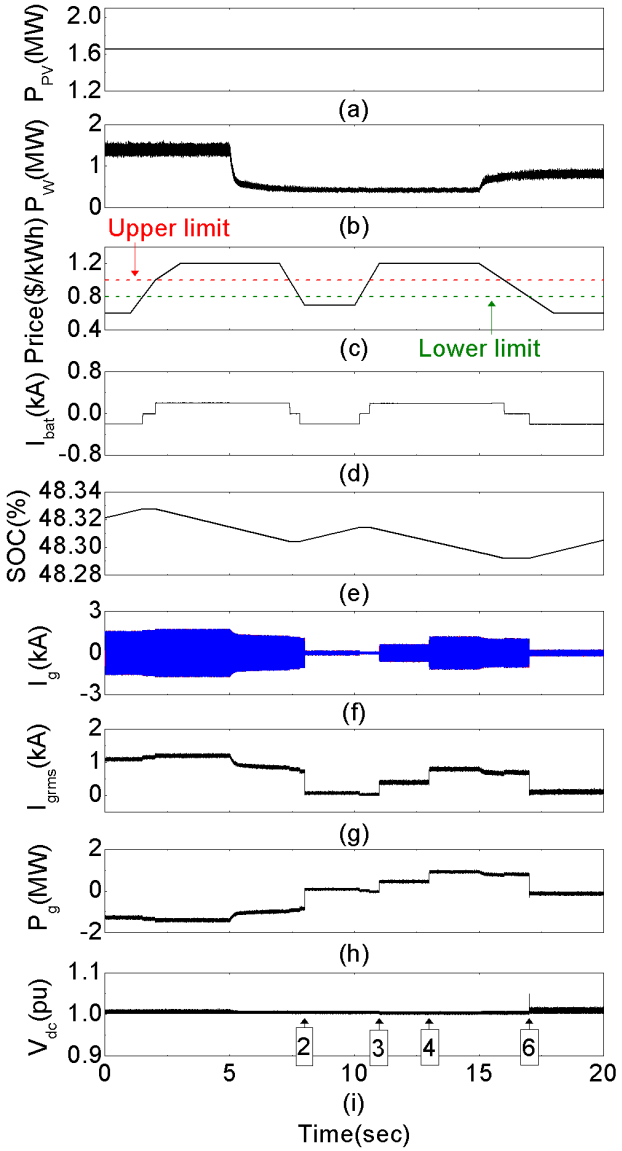

Fig. 10. Grid-connected performance under variable wind power and load demand condition using proposed method.

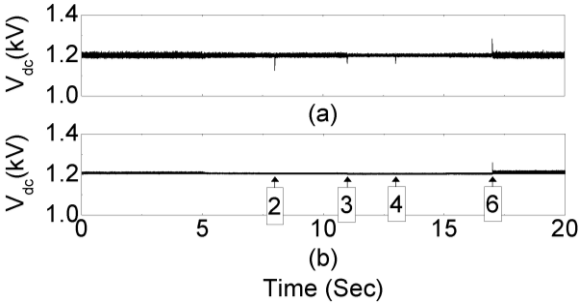

Fig. 11. Comparison of the dc-bus voltage in grid-connected mode. (a) traditional method, (b) proposed method.

appliances at home like washing machines and TVs. Once the SOC drops to SOC_min, non-critical loads will be first switched off. If the SOC still hits the bottom at SOC_min, critical loads will then be cut off subsequently. It is worth mentioning that, to achieve economic load shedding, sophisticated load management algorithm is needed. This requires advanced information communication technology with smart meters, which is out of the scope of this paper.

2) High wind and irradiation and light load

TABLE III Events during islanded operation.

Events	Operations	Time (s)
1	Solar irradiation ramps up	5
2	Load 1 switched in	9
3	Solar irradiation ramps down	11
4	Load 2 and 4 switched in	11
5	Load 4 switched out (load shedding)	12

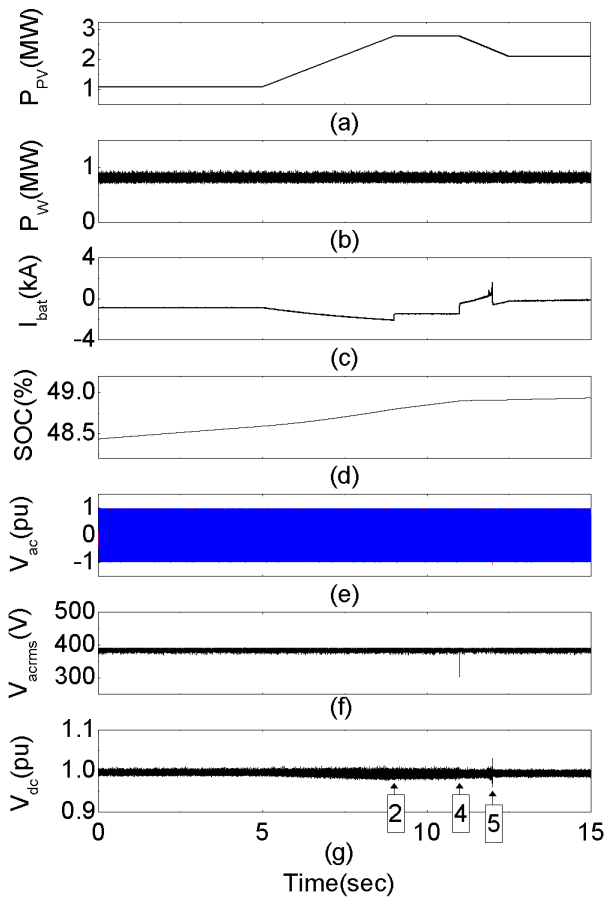

Fig. 12. Islanded performance under variable PV power and load demand condition using proposed method.

Under this circumstance, the generation from PV and wind is greater than the load demand. The ESS is used to absorb the excessive energy by charging the battery. If the power absorbed by the battery exceeds the power rating of the battery or the SOC reaches the maximum value, Off-MPPT operation of the PV and wind systems are needed.

C. Mode 3 operation

This mode corresponds to grid synchronization and connection. Under this mode, the terminal voltage of the ac subgrid starts to track the utility voltage. When the voltages match each other, grid connection can be carried out. To a certain extent, this mode can be regarded as the extension of Mode 2. Similar to Mode 2, the dc-bus voltage relies on ESS and the ac-bus voltage is provided by the interlinking converter.

V. Verification

The microgrid shown in Fig. 1 is modelled and implemented in MATLAB/Simulink. The system parameters are listed in Table I. Load 1 and 2 are linear loads represented by using constant resistances. Load 3 and 4 are modelled as a constant power type representing nonlinear load. Traditional outer voltage and inner current feedback loops with PI regulators are used in comparison with the proposed method (MPCP&MPVP). For a fair comparison,

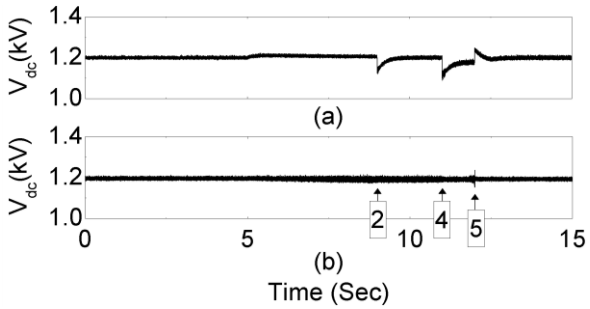

Fig. 13. Comparison of the dc-bus voltage in islanded mode. (a) traditional method, (b) proposed method.

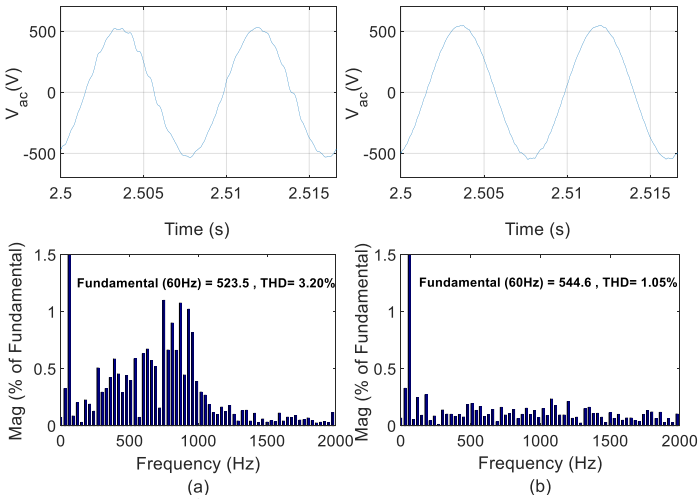

Fig. 14. Comparison of the ac-bus voltage in islanded mode. (a) traditional method, (b) proposed method.

the switching frequencies of the converters are the same for traditional method and the proposed method. To achieve this, the sampling frequency of the MPC is 20kHz, resulting in around 2.0kHz switching frequency at both operation modes for the dc-dc converter, and leading to an about 10kHz switching frequency in grid-connected mode and an around 3kHz switching frequency in islanded operation for the interlinking converter, respectively.

A. Mode 1 operation: Grid-connected

Under grid-connected operation, both the PV and the wind generator are operated in MPPT. The battery operation is determined by the actual electricity price, and the charging/discharging rate is regulated flexibly according to the actual SOC, as explained in Section IV. In order to demonstrate the effectiveness of the proposed control schemes and the reliable operation, a series of events have been imposed, as shown in Table II. Load 1 is connected to the microgrid initially. The solar irradiation level is kept constant at 600W/m^2, resulting in about 1.6MW power output. The wind speed steps down to 8m/s at 5s and steps up to 10m/s at 15s.

Fig. 10 shows the system performance in different operation events. I_g is the current exchanging with the utility grid, I_{grms} is the RMS value of I_g. Prior to Event 2, the power generated from PV and wind generator is partly stored by ESS while the excess is fed back to the utility. When Event 2 occurs, i.e., Load 3 is switched in, the microgrid started to draw power from utility grid because the power generated from PV and wind generators is slightly less than the demand from the load and the ESS. When the Load 2, 4 and 1 are switched in afterwards, the microgrid imports more power from utility accordingly. During the grid-connected operation, the voltage of the ac subgrid is fixed by the utility, while the voltage of the dc subgrid is maintained successfully by the

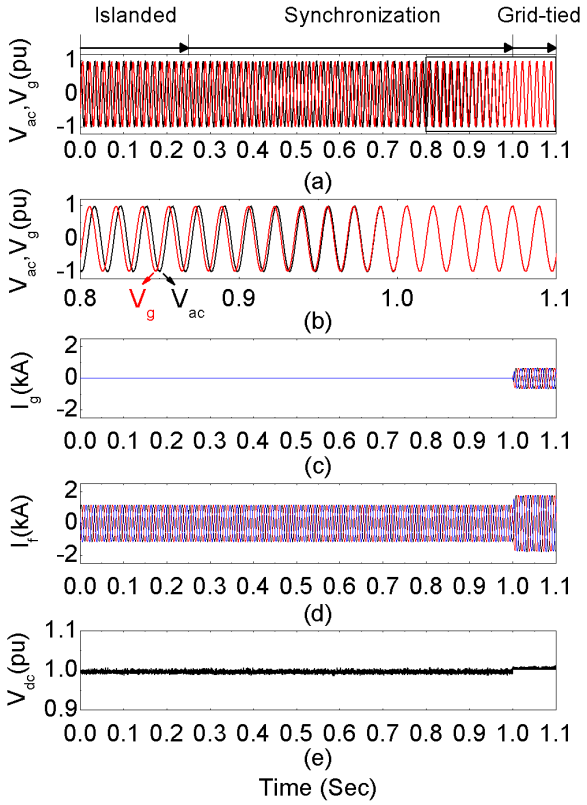

Fig. 15. System performance in grid synchronization and connection using proposed method.

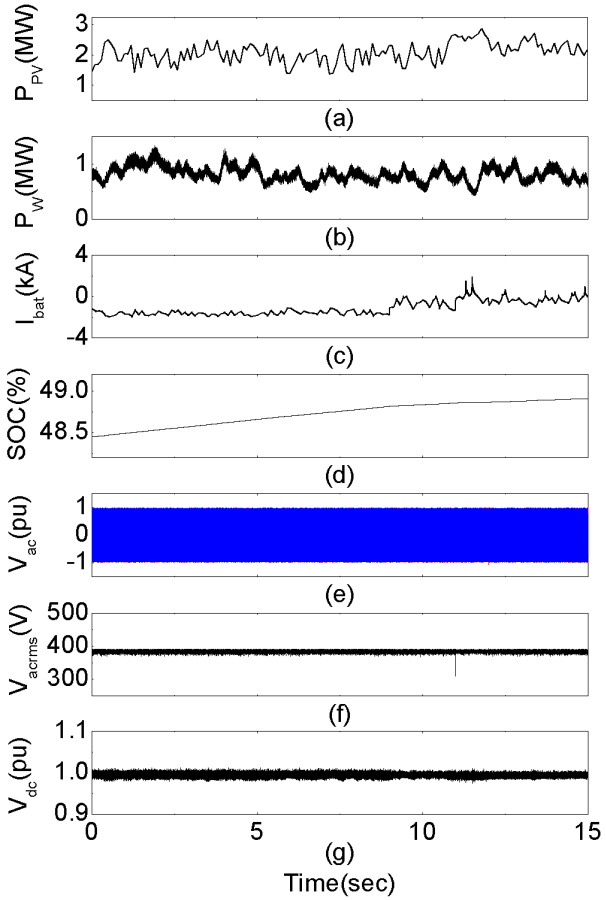

Fig. 16. System performance under real-world solar irradiation and wind speed using proposed method.

ac/dc interlinking converter using MPVP scheme. Fig. 11 compares the dc-bus voltages. It can be seen that, in comparison with traditional PI method, the proposed MPC method can better stabilize the dc voltage with variable generation and consumption.

B. Mode 2 operation: Islanded

Compared to grid-connected operation, islanded mode is more challenging due to the unavailability of the utility system. Thanks to the proposed MPC method and the EMS strategy, the microgrid is able to achieve stable operation and supply high quality electricity, as shown in the follows. In this test, wind speed is fixed at 10m/s, while the solar irradiation varies. Initially, Load 3 (1MW non-linear load) is connected to the ac sugbrid. A variety of events is adopted afterwards, as listed in Table III.

Fig. 12 shows the comprehensive system performance of the microgrid. V_{ac} is the ac bus voltage, V_{acrms} is the RMS value of V_{ac}. Before Event 3 and 4, the generation from PV and wind generator can fully meet the load demand. At 11s, Load 2 and 4 are switched in simultaneously and the PV output started to drop, resulting in ESS discharging to provide additional energy. Since the PV output is decreased gradually, the ESS increased its output accordingly to fill the gap between generation and consumption until it approximatively reached its rated current near 12s. After that, load shedding strategy is activated by switching out the non-critical Load 4.

Since the dc-bus voltage and ac-bus voltage are important aspects to evaluate the microgrid performance in islanded operation, its zoom-in waveform is plotted out in Fig. 13 and Fig. 14 to obtain a better observation. It can be seen that the dc-bus voltage by using traditional PI approach presents obvious oscillations during the transient of load connection/disconnection, whereas the dc-bus voltage by using the proposed method can be better maintained for the same condition. In the ac side of the microgrid, the proposed method also results in better voltage quality. Specifically, the ac voltage is sinusoidal and tightly controlled using MPVP, and its harmonic spectrum is clean with only 1.05% THD, as shown in Fig. 14(b).

C. Mode 3 operation: Grid synchronization and connection

Existing research seldom mentions the grid synchronization and connection of the hybrid ac/dc microgrids, which will be studied here. Fig. 15 shows the detailed results by using the proposed method. Initially the microgrid operated at islanded mode. I_f is the current flowing through the L filter. The grid synchronization algorithm starts to operate at 0.25s and the microgrid is connected to utility grid at 1s. It can be seen that the ac terminal voltage of the microgrid is able to track the utility grid voltage in a short time. It is also seen that no major overshoots of currents are observed. These prompts fast and smooth grid synchronization and connection operation.

D. Microgrid performance under real-time solar irradiance and wind profile

To verify the proposed method with practical consideration, the real-world solar irradiation and wind profiles on Hong Kong Lamma Island [30] are utilized for generating PV output and wind generator output, which are plotted in Fig. 16(a) and (b). The load demand shown in Table III is applied. The microgrid performance in autonomous mode under such fluctuating power generation and consumption is presented in Fig. 16(c)-(g). As can be seen, the battery charges or discharges properly to fill the power gap between the generation and consumption, which can be demonstrated by the battery current and the SOC. The dc-bus voltage is maintained by the BESS using MPCP, while stable ac voltage is generated by the ac-dc interlinking converter using

MPVP scheme.

VI. Conclusion and Future Work

In this paper, a model predictive control strategy of a microgrid with PV-wind-battery sources is proposed. A model predictive current and power (MPCP) scheme is developed to control the bidirectional dc-dc converter in the battery energy storage system (BESS), while a model predictive voltage and power (MPVP) method is proposed to control the ac/dc interlinking converter. They are used to coordinately control the dc/dc converter and ac/dc converter to smooth the renewable energy outputs and maintain dc- and ac-buses voltages. At the system level, a comprehensive energy management scheme is developed to ensure stable operation under different operation modes. The effectiveness of the proposed method is validated based on a pv-wind-battery system with real-world solar and wind profiles, showing better control capability and improved voltage quality in comparison with traditional method.

It should be noted that, compared to traditional cascade control with PID regulators, additional measurements are needed for the proposed MPCP and MPVP approaches. Thus, additional sensors and communication facilities are required. In addition, connection or disconnection of filter capacitors in operation mode transition may cause current spike in practice. These are the issues need to be further addressed in future work.

Acknowledgment

The authors would like to thank the anonymous reviewers for their insightful comments and valuable suggestion on this work.

References

[1] K. H. Ang, G. Chong and Y. Li, "PID control system analysis, design, and technology," *IEEE Trans. Control Syst. Technol*., vol. 13, no. 5, pp. 1813–1827, Sep. 2014.

[2] Y. Han, H. Li, P. Shen, E. Coelho, and J. M. Guerrero, "Review of active and reactive power sharing strategies in hierarchical controlled microgrids," in *IEEE Trans. Power Electron.*, vol. 32, no. 3, pp. 2427-2451, Mar. 2017.

[3] H. Han, X. Hou, J. Yang, J. Wu, M. Su, and J. M. Guerrero, "Review of power sharing control strategies for islanding operation of ac microgrids," in *IEEE Trans. Smart Grid*, vol. 7, no. 1, pp. 200-215, Jan. 2016.

[4] J. M. Guerrero, L. G. de Vicuna, J. Matas, M. Gastilla, and J. Miret, "A wireless controller to enhance dynamic performance of parallel inverters in distributed generation systems," IEEE Trans. Power Electron., vol. 19, no. 5, pp. 1205-1213, 2004.

[5] H. Mahmood, D. Michaelson, and J. Jiang, "Accurate reactive power sharing in an islanded microgrid using adaptive virtual impedances," IEEE Trans. Power Electron., vol. 30, no. 3, pp. 1605-1617, 2015.

[6] A. Micallef, M. Apap, and et al, "Reactive power sharing and voltage harmonic distortion compensation of droop controlled single phase islanded microgrids," IEEE Trans. Smart Grid., vol. 5, no. 3, pp. 1149-1158, 2014.

[7] Y. Shan, J. Hu, Z. Li, and J. M. Guerrero, "A model predictive control for renewable energy based ac microgrids without any PID regulators," *IEEE Trans. Power Electron.*, vol. 33, no. 11, pp. 9122-9126, Nov. 2018.

[8] X. Liu, P. Wang, and P. C. Loh, "A hybrid ac/dc microgrid and its coordination control", *IEEE Trans. Smart Grid*, vol. 2, no. 2, 278-286, Jun. 2011.

[9] A. Merabet, K. T. Ahmed, H. Ibrahim, R. Beguenane, and A. Ghias, "Energy management and control system for laboratory scale microgrid based wind-pv-battery," *IEEE Trans. Sustain. Energy*, vol. 8, no. 1, pp. 145–154, Jan. 2017.

[10] N. Eghtedarpour and E. Farjah, "Power control and management in a hybrid ac/dc microgrid," in *IEEE Trans. Smart Grid*, vol. 5, no. 3, pp. 1494-1505, May 2014.

[11] T. Ma, M. H. Cintuglu, and O. A. Mohammed, "Control of hybrid ac/dc microgrid involving energy storage and pulsed loads", *IEEE Trans. Ind. Appl*., vol. 53, no. 1, 567-575, 2017.

[12] F. Nejabatkhah and Y. W. Li, "Overview of power management strategies of hybrid ac/dc microgrid", *IEEE Trans. Power Electron*., vol. 30, no. 12, 7072-7089, Dec 2015.

[13] S. Vazquez *et al*., "Model Predictive Control: A Review of Its Applications in Power Electronics," *IEEE Ind. Electron. Mag.*, vol. 8, no. 1, pp.16-31, 2014.

[14] D. E. Quevedo, R. P. Aguilera, M. A. Perez, P. Cortes and R. Lizana, "Model Predictive Control of an AFE Rectifier With Dynamic References," in *IEEE Trans. Power Electron.*, vol. 27, no. 7, pp. 3128-3136, July 2012.

[15] J. Hu J. Zhu, and D. G. Dorrell, "Model predictive control of grid-connected inverters for PV systems with flexible power regulation and switching frequency reduction," *IEEE Trans. Industry Applications*, vol. 51, no. 1, pp. 587-594, Jan./Feb. 2015.

[16] X. Li, H. Zhang, M. B. Shadmand, R. S. Balog, "Model predictive control of a voltage-source inverter with seamless transition between islanded and grid-connected operations," IEEE Trans. Ind. Electron., vol. 64, no. 10, pp. 7906–7918, 2017.

[17] A. Parisio, E. Rikos, and L. Glielmo, "A model predictive control approach to microgrid operation optimization," *IEEE Trans. Control Syst. Technol*., vol. 22, no. 5, pp. 1813–1827, Sep. 2014.

[18] A. Ouammi, H. Dagdougui, L. Dessaint, and R. Sacile, "Coordinated model predictive-based power flows control in a cooperative network of smart microgrids," IEEE Trans. Smart Grid, vol. 6, no. 5, pp. 2233–2244, Sep. 2015.

[19] C. Sundstrom, D. Jung, and A. Blom, "Analysis of optimal energy management in smart homes using mpc", in Proc. of *European Control Conf.*, 2016, pp. 2066-2071.

[20] M. Lei, and et al, "An MPC-based ESS control method for PV power smoothing applications", *IEEE Trans. Power Electron*., vol. 33, no. 3, 2136-2144, 2018.

[21] T. Dragicevic, "Model predictive control of power converters for robust and fast operation of ac microgrids", *IEEE Trans. Power Electron*., vol. 33, no. 7, 6304-6317, 2018.

[22] G. M. Masters, "Renewable and efficient electric power systems", John Wiley & Sons, 2004.

[23] R. H. Lasseter, "Smart distribution: coupled microgrids", *IEEE Proceedings*, vol. 99, no. 6, 1074-1082, June 2011.

[24] D. E. Olivares, and et al, "Trends in microgrid control", *IEEE Trans. Smart Grid*, vol. 5, no. 4, 1905-1919, July 2014.

[25] E. Şanal, P. Dost and C. Sourkounis, "LCL-Filter design for a battery charger based on buck converter (DCDC converter)," *2016 IEEE International Conference on Renewable Energy Research and Applications (ICRERA)*, Birmingham, 2016, pp. 617-621.

[26] P. Cortes, et al, "Model predictive control of an inverter with output LC filter for UPS applications," IEEE Trans. Ind. Electron., vol. 56, no. 6, pp. 1875–1883, 2009.

[27] J. Hu, J. Zhu, and D. G. Dorrell, "Model predictive control of inverters for both islanded and grid-connected operations in renewable power generations," *IET Renewable Power Generation*, vol. 8, no. 3, pp. 240-248, April 2014.

[28] Yaramasu V, Wu B, Rivera M, et al, "Enhanced model predictive voltage control of four-leg inverters with switching frequency reduction for standalone power systems", in *Proc. of IEEE Power Electronics and Motion Control Conference (EPE/PEMC)*, 2012.

[29] J. Hu, Y. Xu, K. W. Cheng, J. M. Guerrero, "A model predictive control strategy of pv-battery microgrid under variable power generations and load conditions," *Appl. Energy*, vol. 221, pp. 195-203, Jul. 2018.

[30] https://www.hkelectric.com/en/our-operations/lamma-wind-power-station

Yinghao Shan (S'18) received his M.E. degree in Power Electronics and Electric Drives from Sun Yat-sen University, Guangzhou in 2017. He is currently working toward the Ph.D. degree at Hong Kong Polytechnic University. His research interests include intelligent control algorithm and microgrids.

Jiefeng Hu (S'12–M'14–SM'16) received the Ph.D. degree in electrical engineering from University of Technology Sydney (UTS), Australia, in 2013. From 2011 to 2013, he was involved in the research of minigrids in Commonwealth Scientific and Industrial Research Organization (CSIRO), Newcastle, Australia. Currently he is an Assistant Professor at Hong Kong Polytechnic University, Hong Kong. He served as committee member and session chair in several international conferences such as International Conference on Electrical Machines and System (ICEMS 2017) in Sydney and IET International Conference on Advanced Power System Control,

Operation and Management (APSCOM 2018) in Hong Kong. His research interests include power electronics, renewable energy, and smart microgrids.

Ka Wing Chan (M'98) received the B.Sc. (Hons) and Ph.D. degrees in electronic and electrical engineering from the University of Bath, U.K., in 1988 and 1992, respectively. He currently is an Associate Professor and Associate Head in the Department of Electrical Engineering of the Hong Kong Polytechnic University. His general research interests include power system stability, analysis and control, power grid integration, security, resilience and optimization, demand response management, etc.

Qing Fu received the Ph.D. degree in electrical engineering from Central South University, Changsha, China in 2005. He currently is an Associate Professor at Sun Yat-sen University. He is also the director of Guangdong Engineering Research Center for Green Power Conversion and Intelligent Control. His general research interests include solar inverters and control.

Josep M. Guerrero (S'01-M'04-SM'08-FM'15) received the B.S. degree in telecommunications engineering, the M.S. degree in electronics engineering, and the Ph.D. degree in power electronics from the Technical University of Catalonia, Barcelona, in 1997, 2000 and 2003, respectively. Since 2011, he has been a Full Professor with the Department of Energy Technology, Aalborg University, Denmark, where he is responsible for the Microgrid Research Program (www.microgrids.et.aau.dk). From 2014 he is chair Professor in Shandong University; from 2015 he is a distinguished guest Professor in Hunan University; and from 2016 he is a visiting professor fellow at Aston University, UK, and a guest Professor at the Nanjing University of Posts and Telecommunications.

His research interests is oriented to different microgrid aspects, including power electronics, distributed energy-storage systems, hierarchical and cooperative control, energy management systems, smart metering and the internet of things for AC/DC microgrid clusters and islanded minigrids; recently specially focused on maritime microgrids for electrical ships, vessels, ferries and seaports. Prof. Guerrero is an Associate Editor for a number of IEEE TRANSACTIONS. He has published more than 450 journal papers in the fields of microgrids and renewable energy systems, which are cited more than 30,000 times. He received the best paper award of the IEEE Transactions on Energy Conversion for the period 2014-2015, and the best paper prize of IEEE-PES in 2015. As well, he received the best paper award of the Journal of Power Electronics in 2016. During five consecutive years, from 2014 to 2018, he was awarded by Thomson Reuters as Highly Cited Researcher. In 2015 he was elevated as IEEE Fellow for his contributions on "distributed power systems and microgrids."